

## PERFORMANCE CHARACTERIZATION OF THE TRW 35K PULSE TUBE COOLER

S. A. Collins, D. L. Johnson, G. T. Smedley, and R. G. Ross, Jr.

Jet Propulsion Laboratory  
California Institute of Technology  
Pasadena, CA 91109

### ABSTRACT

The TRW 35K pulse tube cooler is **configured** as an integral cooler, with the pulse tube attached perpendicular to a pair of compressors operating into a common compression chamber. The cooler was optimized for 35K operation and has a nominal cooling capacity of 850 **mW** at 35 K with a cooler input power of 200 W. It also provides 2 W of cooling at 60 K for 90 W of input power. The cooler was extensively characterized by JPL, measuring the thermal performance and the cooler-generated vibration and EMI as a function of piston stroke and offset position. The thermal performance was found to be quite sensitive to the piston offset position. The pulse tube parasitic conduction levels were also **measured** and shown to have a strong angular dependence relative to gravity. Magnetic shielding studies were performed to examine radiated magnetic emission levels from compressors with and without shielding.

### INTRODUCTION

As part of JPL's **cryocooler** characterization program sponsored jointly by the Air Force Phillips Laboratory and the NASA Earth Observing System **AIRS** Instrument Project, the TRW 35K pulse tube cooler was recently characterized in terms of its refrigeration performance, generated vibration, and electromagnetic compatibility. The results of these performance measurements are summarized in this paper.

The TRW 35K pulse tube cooler is an integral cryocooler that consists of a pair of flexure-bearing compressors operating on a common compression chamber ported to a pulse-tube cold head. The cold head is mounted perpendicular to the compressor axis in the center of the compressor assembly, as shown in Figure 1. Additional details can be found in Reference 1.

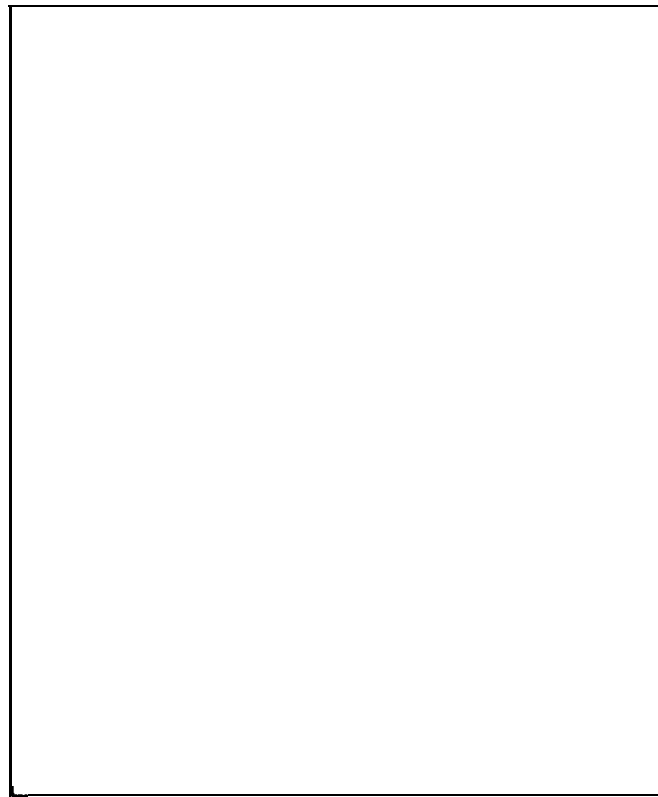


Figure 1. TRW 35K **pulse** tube cooler.

## REFRIGERATION PERFORMANCE

Refrigeration performance measurements were conducted in the **JPL** thermal-vacuum test facility that is used to simulate conditions in space and to provide a highly stable thermal test environment; the high level of **environmental** stability allows the accurate and repeatable measurements that are necessary to illuminate subtle and important performance sensitivities. The cooler's heatsink temperature was regulated by attaching a pair of copper heat exchangers with a temperature-controlled fluid loop to the mechanical flats on either side of the cooler's **centerplate**. The heat exchangers were thermally isolated from the vacuum housing and also served as the cooler's structural supports. The cooler's **coldblock** was outfitted with a **cryodiode** to measure the **coldblock** temperature and a wire-wound heater to apply a heat load. The **coldblock** was then wrapped in several layers of aluminized Kapton **MLI** to reduce any parasitic radiation heat load to negligible levels, and the vacuum was maintained below  $10^{-6}$  torr to avoid gaseous conduction effects.

The cooler was driven using a low-distortion audio amplifier with a sinusoidal voltage waveform. The power to the cooler was monitored using a **true-RMS** power meter.

Sensitivity studies were conducted with respect to key operational and environmental parameters such as compressor stroke, piston offset, drive frequency, and heatsink temperature. No attempt was made to optimize the cooler's performance in any one test; the parameter values were selected to allow sufficient variation to observe performance sensitivity while restricting the input power to less than 200 W.

### Thermal Performance

The thermal performance of the TRW 35K cooler is presented in a multivariable format that depicts the interrelationship between the input power, the **coldblock** load, the specific power, the **coldblock** temperature, and a sensitivity parameter. For example, Figure 2 maps the

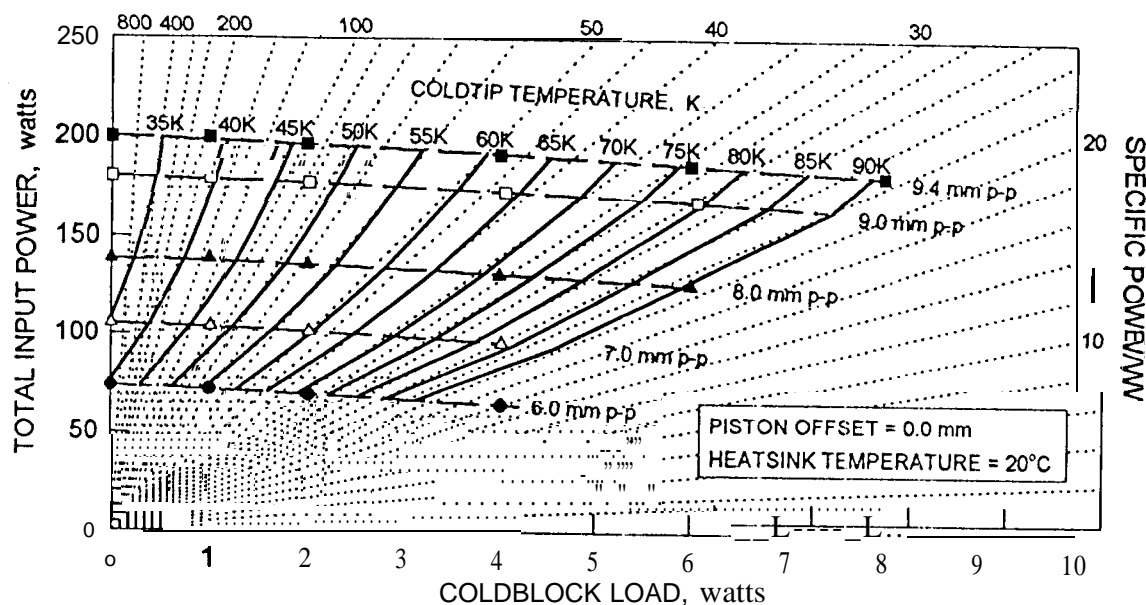


Figure 2. Sensitivity of thermal performance to compressor stroke.

performance as a function of compressor stroke. At each compressor stroke, measurements were made at several coldblock loads. A curve fit through these data yields a constant-stroke load line. Interpolation is then used to find the performance at a particular coldblock temperature, allowing isotherms to be developed across the sensitivity parameter, e.g. the compressor stroke. The slope of the isotherms may be compared to the specific-power grid lines to determine whether a particular change in the sensitivity parameter yields better or worse performance with regard to overall refrigeration efficiency.

Figure 2 shows the sensitivity of the cooler's thermal performance to compressor stroke with no piston offset and with a heatsink temperature of 20°C. The input power is strongly dependent on the compressor stroke and weakly dependent on the coldblock load. It is worth noting that very good performance is achieved over much of the parameter space: the isotherms are parallel to the specific-power grid lines over a wide range of coldblock loads, coldblock temperatures, and compressor strokes. Thus, at a particular coldblock temperature, the compressor stroke can be adjusted to accommodate a range of coldblock loads with little change in refrigeration efficiency.

The efficiency of the cooler may be improved by reducing the compression chamber's dead volume. Figure 3 shows the sensitivity of the thermal performance to piston offset with a compressor stroke of 9.0 mm<sub>pp</sub> and a heatsink temperature of 20°C. As the offset increases from -1.0 mm to +2.0 mm, which moves the pistons toward one another, more input power is required to maintain a given stroke and the cooling capacity at a given temperature is increased. The cooler is, however, operating more efficiently at the higher offsets: notice that the isotherms are less steeply sloped than the specific-power grid lines,

## Cooler Efficiency

An important figure-of-merit for cryocoolers is the thermodynamic coefficient of performance (COP) of the refrigerator expressed as a percentage of the ideal Carnot COP, which is uniquely defined in terms of the coldblock temperature and the heatsink temperature. The thermodynamic COP is a measure of the cooler's ability to convert work done on the gas into net cooling power. In the data presented here, the work done on the gas is approximated as the input electrical power minus the drive-motor  $i^2R$  losses.

Figure 4 shows the measured % Carnot COP as a function of the coldblock temperature; the sensitivity to compressor stroke is also shown. Notice that larger strokes achieve colder no-

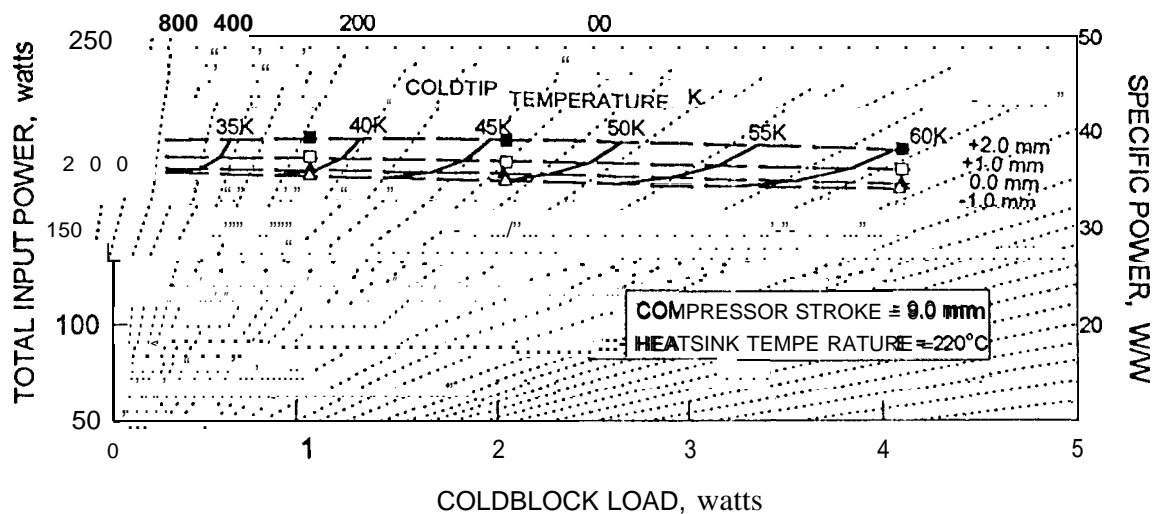


Figure 3. Sensitivity of thermal performance to piston offset.

load temperatures but appear to peak at lower % Carnot COP values than do the smaller strokes, as is also seen with Stirling coolers.<sup>2</sup>

The performance of the cooler drive motors was assessed: the motor efficiency was approximately 85% and the power factor was near 0.96. This performance was typical over a broad range of operational parameters, which contributes to the cooler's high refrigeration efficiency at a variety of operating points.

### Off-State Conductance

Cold-head conductive losses can significantly reduce the amount of useful cooling work that a cooler can perform. These losses can also represent a major heat load in cryogenic applications that include redundant or non-operating coolers. The off-state conductance was measured using an equilibrium technique described in Reference 3. The 35K pulse tube cooler is physically quite large, and the coldblock is located in the middle of the coldhead, resulting in a relatively high conductive heat load of 500 mW at 35 K.

The off-state heat load can be significantly enhanced under certain orientations of the cold head with respect to gravity, as the hollow pulse tube becomes a source of convective helium gas flow. This is shown dramatically in Figure 5. Off-state heat loads in excess of 2000 mW were measured when the cold head was horizontal. The convective effect was highly sensitive to

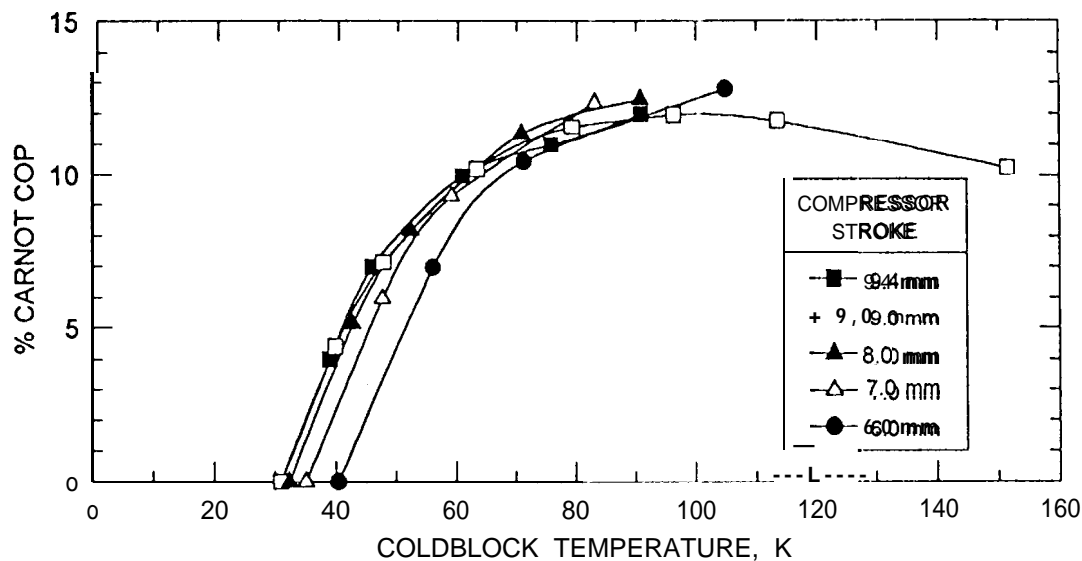


Figure 4. Sensitivity of % Carnot COP to compressor stroke.

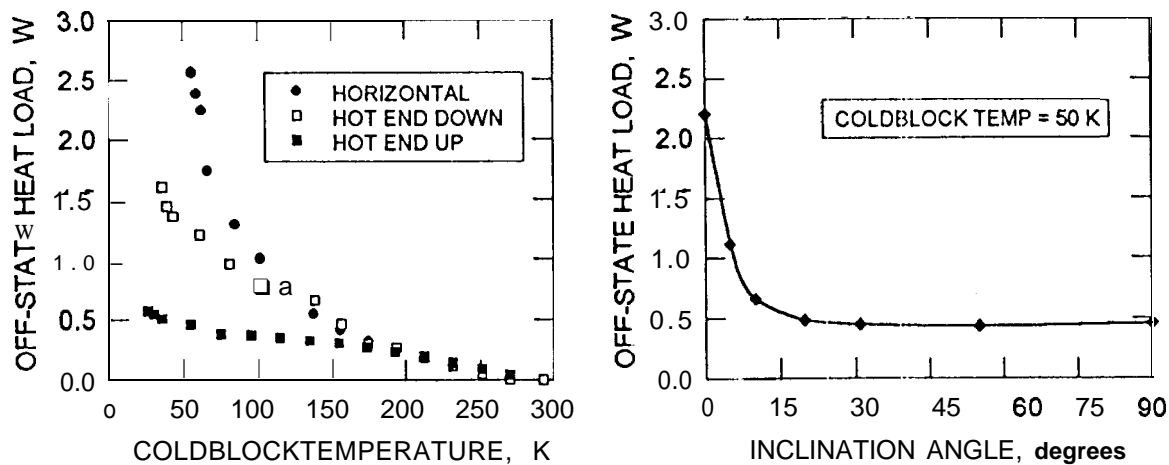


Figure 5. Sensitivity of off-state conductance to orientation.

coldhead inclination, with 20° of inclination being sufficient to eliminate the enhanced heat flow. This is an important consideration when planning the ground-testing of cryogenic systems with non-operating cryocoolers.

## GENERATED VIBRATION

Measurements of the vibration generated by the TRW 35K pulse tube cooler were conducted in the JPL cryocooler vibration characterization facility using a special-purpose six-degree-of-freedom dynamometer. This dynamometer has a frequency range from 10 to 500 Hz and a force sensitivity from 0.005 N to 450 N full scale. During operation, the generated forces are simultaneously recorded in real time using a spectrum analyzer.

### Integral Cooler Forces

As this cooler features a back-to-back compressor configuration, the vibration along the compressor axis at the drive frequency was minimized by trimming the stroke of one of the two compressors. The resulting forces are shown in Figure 6. The z-axis is the compressor axis, the x-axis is the cold-head axis, and the y-axis completes the orthogonal set. Most of the harmonics have amplitudes of 0.1 to 1 N, and many of them display little sensitivity to compressor stroke. Notice that the axial ( $F_z$ ) and the lateral ( $F_x$  and  $F_y$ ) vibrations are of similar amplitudes. These vibration levels are comparable to those generated by back-to-back Stirling coolers.<sup>4</sup>

### Split Cooler Forces

In order to gain greater insight into the vibration generated by the pulse-tube cold head, a split cooler was also tested on the JPL dynamometer. The compressors and the cold head were provided by TRW and were similar to the 35K cooler, but they were not mated in the integral configuration. Figure 7 depicts the coldhead-generated forces. In this figure, the z-axis is "the cold-head axis, the y-axis is defined by the transfer lines coupling the cold head to the compressors, and the x-axis completes the orthogonal set. The forces are shown as a function of the pressure-wave amplitude. Notice that the cold head is not free of vibration, although the levels are significantly smaller than the integral cooler's vibration.

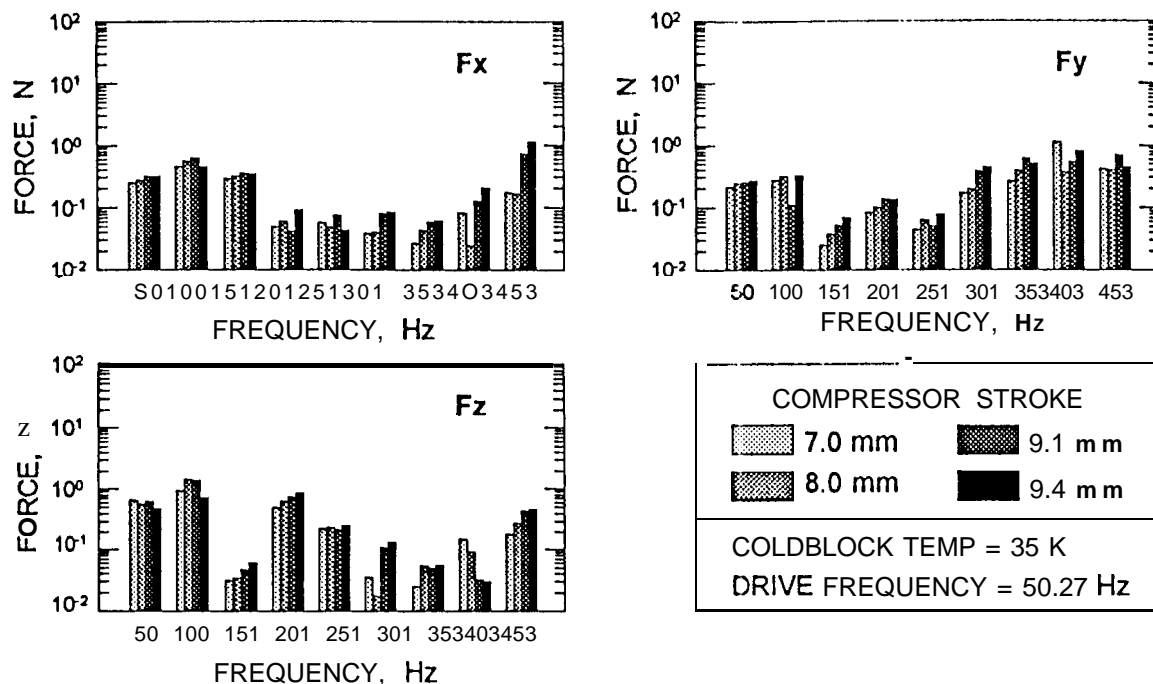


Figure 6. Sensitivity of generated vibration to compressor stroke.

### Coldblock Motion

In addition to the vibration generated by the compressors and the cold head, the motion of the coldblock itself can act as a disturbance. This motion was measured with the integral cooler mounted on the dynamometer, providing a rigid mount for the cooler. A set of three accelerometers was then attached to the coldblock; they were aligned to the same axes described for Figure 6 (the z-axis is the compressor axis and the x-axis is the cold-head axis). The measurements are shown in Figure 8. Notice that the motion is significantly greater along the cold-head axis than it is in the other two directions. These displacements are comparable in amplitude to the coldtip motion of Stirling coolers.<sup>5</sup>

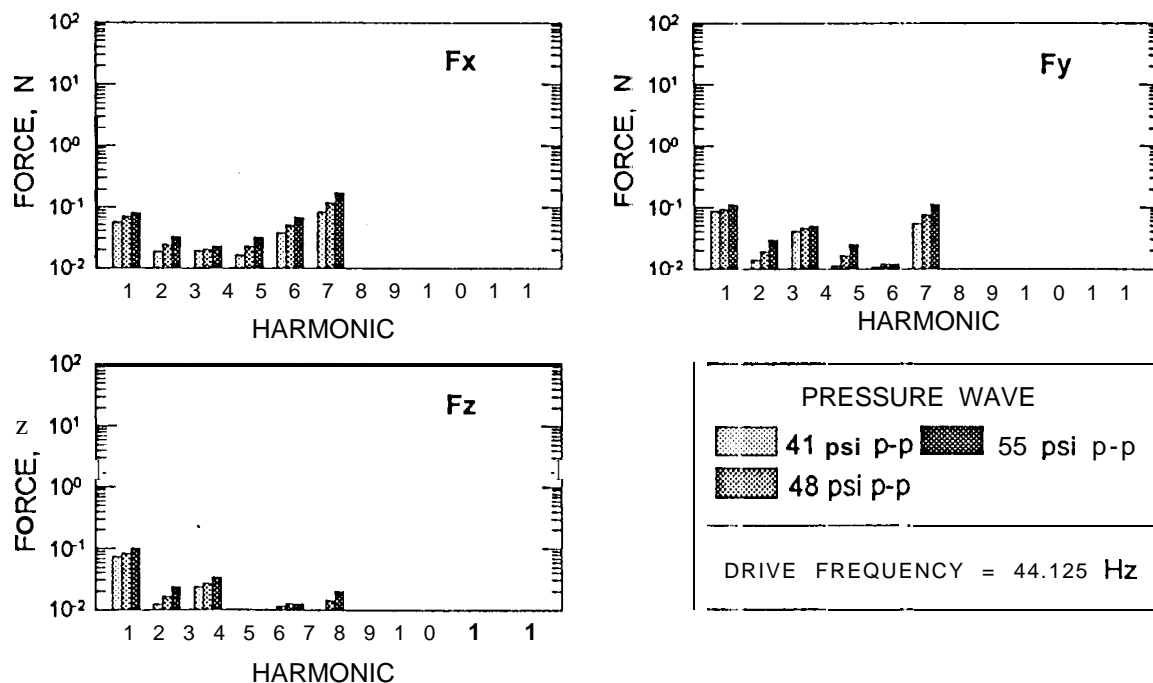


Figure 7. Sensitivity of cold-head vibration to pressure amplitude.

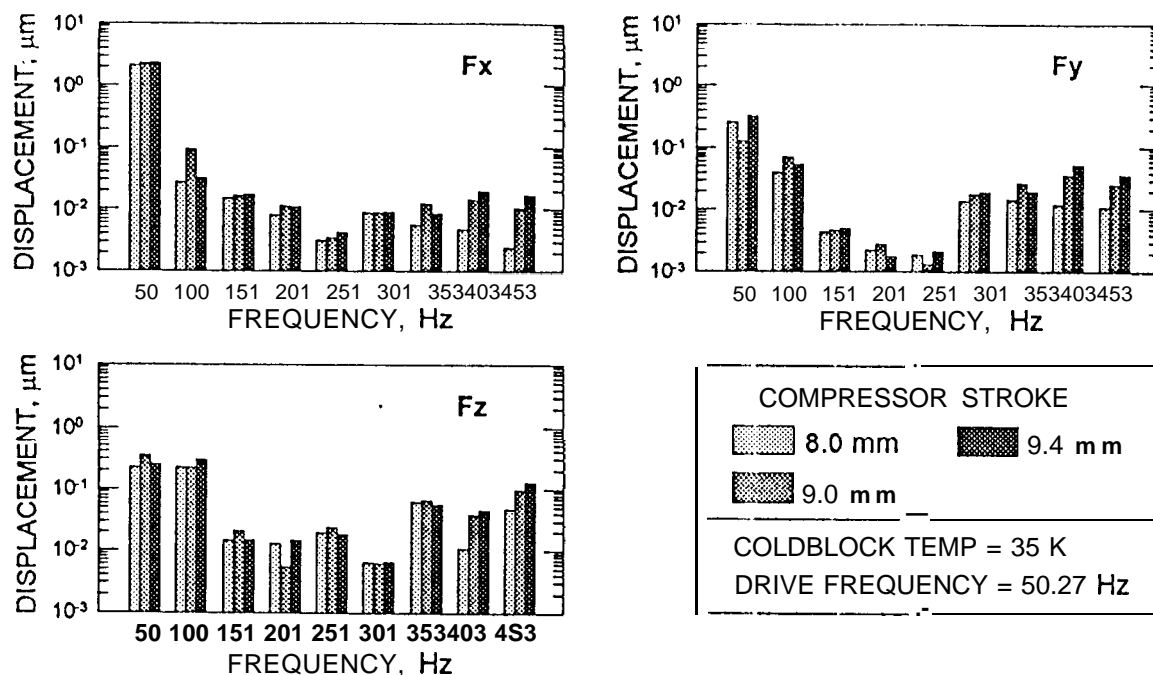


Figure 8. Sensitivity of coldblock motion to compressor stroke.

## ELECTROMAGNETIC COMPATIBILITY

EMC measurements were made with the cooler placed in a steel RF-shielded room and grounded to a copper-laminated table. During the testing the drive electronics were placed in an adjacent area outside the shielded room with connecting cabling fed through a bulkhead in the wall. The cabling was sheathed in aluminum foil and grounded to the copper table top to minimize any contributing radiation.

Measurements of the cooler-generated AC electric and magnetic field emissions were made. The cooler was operated at full power to create worst-case emissions. The cooler was powered with linear-amplifier power supplies, so the measurements did not contain the high-frequency EMI that is typical of the high-efficiency PWM-type power converters used in spacecraft applications. For the most part, the radiated AC electric field emissions were well below the specification limits of MIL-STD 461 C: RE 02. The AC magnetic field emissions were measured at distances of 7 cm and 1 m from the cooler. The specification limits of MIL-STD 461 C: RE 01 and RE 04 were exceeded by the first three harmonics of the cooler drive frequency, which is typical for cooler compressors of this size.<sup>6</sup>

The spatial distribution of the AC magnetic field emitted from the compressors was mapped in both the axial and radial directions. Figure 9 depicts the field distribution and strength (in nT) based on the magnitude of the fundamental. The measurements were then repeated with 0.030", thick p-metal shielding wrapped around each compressor housing. As the figure indicates, the shielding had a significant effect on the intensity of the AC magnetic field emissions.

The DC magnetic field of the cooler was mapped. For these measurements the cooler was disconnected from the drive electronics and was mounted inside a set of DC coils that generate a magnetic field to cancel the earth's magnetic field within the test volume. The magnitude of the cooler's DC magnetic field was found to be 200 milligauss at a distance of 0.5 m.

## SUMMARY

The TRW 35K pulse tube cooler was recently characterized at JPL in terms of its refrigeration performance, generated vibration, and electromagnetic compatibility. Sensitivity studies were conducted with respect to key operational and environmental parameters such as

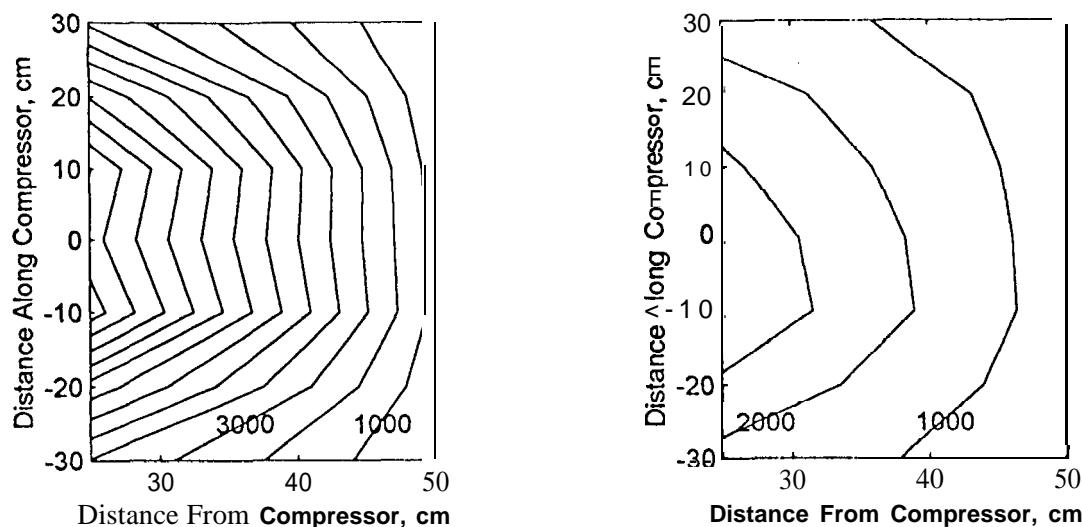


Figure 9. Effect of shielding on AC magnetic field emissions. The contour spacing is 1000 nT.

compressor stroke, piston offset, drive frequency, and heatsink temperature. The thermal performance was found to be quite sensitive to piston offset position, and the off-state heat load was shown to have a strong angular dependence relative to gravity.

## ACKNOWLEDGMENTS

The work described in this paper was carried out by the Jet Propulsion Laboratory, California Institute of Technology, and was sponsored by the Air Force Phillips Laboratory and the NASA EOS AIRS Project. Particular credit is due S. Leland, who provided assistance and support with many of the test setups.

References herein to a particular cooler, or to any specific commercial product, process, or service by tradename, trademark, manufacturer, or otherwise, does not constitute or imply its endorsement by the United States Government or the Jet Propulsion Laboratory, California Institute of Technology.

## REFERENCES

1. W.W. Burt and C.K. Chan, Demonstration of a high performance 35 K pulse tube cryocooler, "Cryocoolers 8," R.G. Ross, Jr., cd., Plenum Press, New York (1995), pp. 313-319.
2. G.T. Smedley, G.R. Men, D.L. Johnson, and R.G. Ross, Jr., Thermal performance of stirling-cycle cryocoolers: a comparison of JPL-tested coolers, "Cryocoolers 8," R.G. Ross, Jr., cd., Plenum Press, New York (1995), pp. 185-195.
3. V. Kotsubo, D.L. Johnson, and R.G. Ross, Jr., Cold-tip off-state conduction loss of miniature stirling cycle cryocoolers, "Advances in Cryogenic Engineering," Vol. 37, Part B, Plenum Press, New York (1992), pp. 1037-1043.
4. G.R. Men, G.T. Smedley, D.L. Johnson, and R.G. Ross, Jr., Vibration characteristics of stirling cycle cryocoolers for space application, "Cryocoolers 8," R.G. Ross, Jr., cd., Plenum Press, New York (1995), pp. 197-208.
5. R.G. Ross, Jr., D.L. Johnson, and V. Kotsubo, Vibration characterization and control of miniature stirling-cycle cryocoolers for space application, "Advances in Cryogenic Engineering," Vol. 37, Part B, Plenum Press, New York (1992), pp. 1019-1027.
6. D.L. Johnson, G.T. Smedley, G.R. Men, R.G. Ross, Jr., and P. Narvaez, Cryocooler electromagnetic compatibility, "Cryocoolers 8," R.G. Ross, Jr., cd., Plenum Press, New York (1995), pp. 209-220.



